Accepted Manuscript

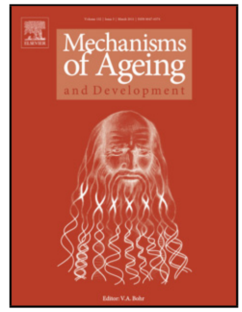

Title: Long-term exposition to a high fat diet favors the appearance of β-amyloid depositions in the brain of C57BL/6J mice. A potential model of sporadic Alzheimer's disease

Author: Oriol Busquets Miren Ettcheto Mercè Pallàs Carlos Beas-Zarate Ester Verdaguer Carme Auladell Jaume Folch Antoni Camins

PII: S0047-6374(16)30085-9
DOI: http://dx.doi.org/doi:10.1016/j.mad.2016.11.002
Reference: MAD 10895

To appear in: *Mechanisms of Ageing and Development*

Received date: 2-6-2016
Revised date: 26-9-2016
Accepted date: 11-11-2016

Long-term exposition to a high fat diet favors the appearance of β-amyloid depositions in the brain of C57BL/6J mice. A potential model of sporadic Alzheimer's disease

Oriol Busquets[1,2,4], Miren Ettcheto [2,4], Mercè Pallàs[2,4,5], Carlos Beas-Zarate [6] Ester Verdaguer[3,4,5], Carme Auladell[3,4,5], Jaume Folch [$1,4] and Antoni Camins [$2,4,5]

[1]Departament de Bioquímica i Biotecnologia, Facultat de Medicina i Ciències de la Salut, Universitat Rovira i Virgili, Reus, Tarragona, Spain.

[2]Departament de Farmacologia, Toxicologia i Quimica Terapeurica, Facultat de Farmàcia i Ciències de l'Alimentació, Universitat de Barcelona, Barcelona, Spain

[3]Departament de Biologia Cel·lular, Fisiologia i Immunologia, Facultat de Biologia, Universitat de Barcelona, Barcelona, Spain.

[4] Biomedical Research Networking Center in Neurodegenerative Diseases (CIBERNED), Madrid, Spain.

[5]Insitutut de Neurociències, Universitat de Barcelona, Barcelona, Spain.

[6]Laboratorio de Regeneración y Desarrollo Neural, Instituto de Neurobiología, Departamento de Biología Celular y Molecular, CUCBA, Guadalajara, México

Correspondence/Reprint request:

Dr. Antoni Camins,

Unitat de Farmacologia i Farmacognòsia, Facultat de Farmàcia, Centros de Investigación Biomédica en Red de Enfermedades Neurodegenerativas (CIBERNED).

Universitat de Barcelona.

Barcelona, Avinguda/Joan XXIII, Spain.

e-mail: camins@ub.edu

Highlights

- High fat diet induced the deposition of the β-amyloid peptide in brain mice
- High fat diet induced a brain neuroinflammatory process
- High fat diet induced a dysregulation in autophagy and apoptosis

Abstract

Aims: The sporadic and late-onset form of Alzheimer's disease (AD) constitutes the most common form of dementia. This non-familiar form could be a consequence of metabolic syndrome, characterized by obesity and the development of a brain-specific insulin resistance known as type III diabetes. This work demonstrates the development of a significant AD-like neuropathology due to these metabolic alterations.

Methods: C57BL/6J mice strain were divided into two groups, one fed with a diet rich in palmitic acid (high-fat diet, HFD) since their weaning until 16 months of age, and another group used as a control with a regular diet. The analyses were carried out in the dentate gyrus area of the hippocampus using a Thioflavin-S stain and immunofluorescence assays.

Results: The most significant finding of the present research was that HFD induced the deposition of the βA peptide. Moreover, the diet also caused alterations in different cell processes, such as increased inflammatory reactions that lead to a decrease in the neuronal precursor cells. In addition, the results show that there were also dysregulations in normal autophagy and apoptosis, mechanisms related to βA formation.

Conclusions: The present findings confirm that HFD favors the formation of βA depositions in the brain, a key feature of AD, supporting the metabolic hypothesis of sporadic AD.

Abbreviations

Aβ: β-amyloid

AD: Alzheimer's disease

AMPK: AMP-activated protein kinase

ANS: Autonomic Nervous System

BACE1: beta-site APP-cleaving enzyme 1

BBB: Brain Blood Barrier

CSF: Cerebrospinal fluid

DIO: Diet-induced obesity

HCD: High calorie diet

HFD: High-fat diet

IGF-1: Insulin-like growth factor-1

MAPK: mitogen-activated protein kinase

PTP1β: Protein tyrosine phosphatase 1β

T2DM: Type 2 diabetes mellitus

Introduction

Diseases like type-II diabetes mellitus (T2DM), atherosclerotic cardiovascular disease and metabolic syndrome are derived from population's life expectancy continuous growth and the worsening of people's life habits. These diseases together with other degenerative conditions have a metabolic origin and are associated with central/upper body fat accumulation, hypertension, dyslipidemia and hyperglycemia (McGill, A.-T., 2014). The development of obesity and metabolic syndrome is related to an excessive consumption of red meats, refined sugars, high fat foods and refined grains that contain high concentrations of saturated and trans-fatty acids (Freeman, 2014; McGill, A.-T., 2014). Metabolic syndrome is one of the most complex and heterogeneous diseases and affects many organs like liver, kidney, gut, pancreas and brain (Hristova, 2013).

Metabolic derangements resulting of obesity cause inflammation, insulin resistance, endoplasmic reticulum stress and impairment of cognitive functions (De Felice 2015); going so far as being related in epidemiological studies to Alzheimer's disease (AD) (Julien, 2010; De Felice & Ferreira, 2014; Grillo, 2015).

Given recent published findings that provide evidence that HFD causes obesity, insulin resistance and aggravates several AD markers, we chose this experimental approach as our method to study the mechanisms that lead to AD progression (Nuzzo, 2015). Previous results from our group in both C57BL/6J and APP/PS1 mice indicate that continuous feeding with HFD, starting at the time of weaning, is sufficient to induce a metabolic syndrome and appears to have direct effects on brain insulin regulation and mitochondrial function. Moreover, through the Morris Water Maze Test (MWM) and the Novel Object Recognition Test (NOR), a significant cognitive decline was evidenced in those animals (Giacco, 2011; Petrov, 2015).

There is growing evidence to believe that obesity as it occurs in aging, promotes low-grade systemic inflammation, including the brain (Tucsek, 2014; Tang, 2015; Pistell, 2010). Macrophages, microvascular endothelial cells and adipocytes release a wide range of inflammatory mediators into the bloodstream, such as C-reactive protein (CRP), tumor necrosis factor-α (TNF-α), interferon-γ (IFN-γ), and interleukin (IL) -6 and -8 (Nousen, 2013). This systemic inflammation, could also affect most cells ability to progress in the cell cycle and, in turn, their ability to generate new ones. The positive or negative effects of pro- and anti-inflammatory cytokines still need for further understanding but is an important point to be assessed (Borsini, 2015; Singh, 2012). The dentate gyrus (DG), a structural and functional part of the hippocampus involved in the formation of memory, is one of the brain areas that shows clear neurogenesis ability, allowing for the formation of new neurons, that later migrate into other areas of the tissue. As it is later glimpsed in this research, this neurogenesis system is indeed negatively affected by the neuroinflammation derived of the development of a metabolic syndrome.

Another cellular mechanism that would be affected by the metabolic syndrome is autophagy (Lipinski, 2010). This cellular process allows for the recycling of cellular components to sustain the viability of cells when they have been outstripped of their exogenous nutrient supply and it allows for the renewal of cellular components. Also, a link exists between insulin resistance and autophagy (Yoshizaki, 2012). As it has been previously reported in several papers through the study of these mechanisms in multiple mice models, the appearance of insulin resistance causes the suppression of autophagy, although the mechanism through which it occurs is yet to be clear. In this line, p53 is a protein identified to be involved in the autophagy program. Autophagy and p53 have a negative feedback loop in which p53 induces autophagy, which then limits p53 activation (Kruiswijk, 2015). The B-cell lymphoma 2 (BCL-2) also regulates autophagy and is part of an interplay in which p53 inhibits BCL-2 through its phosphorylation and, in turn, BCL-2 inhibits several proteins downstream of the activation of p53, like the p53 upregulated modulator of apoptosis (PUMA), the neuro-oncological ventral antigen (NOVA), the BCL-2-like protein 11 known as BIM and the BCL-2-like protein 4 known as BAX (Maiuri, 2010). Moreover, BCL-2 inhibits the BECLIN1, a protein that participates in the formation of the autophagosome (Park, 2009; Lorin, 2010).

Since our group has already published data on several alterations due to short-term feeding of HFD (Petrov, 2015). In the present study, we tried to discern the negative consequences of a long-term feeding on a HFD and its implications in the alteration of multiple cell processes. The results obtained through histochemical stains and immunofluorescence techniques supported the link between metabolic alterations and the appearance of βA deposit together with glial reactivity. The analyses of different proteins related to apoptosis and to autophagy suggested that these alterations would be the result of impairment in cellular process such as apoptosis and autophagy activity. Moreover, the negative impact of the metabolic syndrome would also have consequences on the progression of neurogenesis mechanisms.

Materials and Methods

Animals

16-months old *wild-type* C57BL/6J mice were used in this study. They were separated in two study groups: those fed with regular control diet (CT) and those fed with a HFD. Animals were maintained under standard animal housing conditions with a 12-h dark–light cycle with free access to food and water. Animal procedures were conducted according to ethical guidelines (European Communities Council Directive 2010/63/EU) and approved by the local ethical committee (UB). Every effort was made to minimize animal suffering and to reduce the number of animals used.

Diet

HFD was purchased from Research Diets, Inc. (Product D08061110). It is made out of hydrogenated coconut oil. The contents of this diet are shown in **Table 1**. Both CT and HFD were fed to the animals from their weaning until they were sacrificed at 16 months of age.

Antibodies

The primary and secondary antibodies used in this study have been listed in **Tables 2** and **3**.

Immunofluorescence

Mice used for immunofluorescence studies were anesthetized by intraperitoneal injection of ketamine (d=100mg/kg) and xylazine (d=10 mg/kg) and perfused with 4% paraformaldehyde (PFA) diluted in 0.1M phosphate buffer (PB). Brains were removed and stored in the same solution overnight at 4°C and 24 hours later, they were cryoprotected in 30% sucrose-PFA-PB solution. Coronal sections of 20 µm of thickness were obtained by a cryostat (Leica Microsystems).

On the first day, free-floating sections were washed three times with 0.1 mol/L PBS pH 7.35 and after five times with PBS-T (PBS 0.1 M, 0.2% Triton X-100). Then, they were incubated in a blocking solution containing 10% fetal bovine serum (FBS), 1% Triton X-100 and PBS 0.1M + 0.2% gelatin for 2 hours at room temperature. After that, slices were washed with PBST (PBS 0.1 M, 0.5% Triton X-100) five times for 5 minutes each and incubated with the primary antibody overnight. On the second day, brain slices were washed with PBS-T (PBS 0.1 M, 0.5% Triton X-100) 5 times for 5 minutes and incubated with the appropriate secondary antibody for 2 hours at room temperature. Later, sections were co-stained with 0.1 µg/ml Hoechst 33258 (Sigma-Aldrich, St Louis, MO, USA) for 15 minutes in the dark at room temperature and washed with PBS 0.1M. Finally, the slides were mounted using Fluoromount G (EMS) image acquisition was performed with an epifluorescence microscope fluorescence filter (BX61 Laboratory Microscope, Melville, NY-Olympus America Inc.).

Thioflavin-S Staining

The stain solution was made of Thioflavin-S diluted with PBS 0.1 mol/L on a 0.0033% concentration. Brain coronal sections were incubated for 8 minutes in darkness at room temperature.

Quantification of results

All images and quantifications shown in this paper were obtained from coronal sections from Bregma 1.34 – to Bregma 2.46 mm in the mouse brain. NESTIN and ULK1 positive cells quantification was obtained solely from the DG of at least 3 animals from each experimental group. For plaque quantification, similar and comparable histological areas were selected, focusing on having the hippocampus and the whole cortical area positioned adjacently.

In order to quantify the differential fluorescence relative intensity in the images, ImageJ software was used. Relative intensity quantification numbers were obtained under the following formula: CTCF (Corrected Total Cell Fluorescence) = Integrated Density - (Area of selected cell X Mean fluorescence of background readings).

Statistical Analysis

Statistical analysis was performed with unpaired t-test. Data are presented as means ± SEM, and differences are considered significant at $p < 0.05$ (*), $p < 0.01$ (**), $p < 0.001$ (***) and $p < 0.0001$ (****).

Results

βA peptide accumulation and increased glial reactivity

The presence of βA peptide depositions is a hallmark of AD. Their presence was evaluated through the Thioflavin-S stain, used for the detection of fibrillar aggregates, and using the 12F4 antibody to detect βA diffuse plaques. In both detection methods there was a significant appearance of deposits of the βA peptide in the HFD experimental group versus what occurred in controls (**Figure 1)**.

Two antibodies were used to analyze the glial response in the DG of the brain between those animals fed with CT and HFD. Astrogliosis, a feature observed in different brain pathologies, was identified using an antibody against glial fibrillary acidic protein (GFAP), the main constituent of the intermediate filament system of adult astrocytes, (Pekny, 2014). Also, with an antibody against ionized calcium-binding adapter molecule 1 (Iba1), the morphology of microglial cells was studied. (Deininger, 2002). An augment in astrocyte and microglial response was detected (**Figures 2** and **3).**

Reduction in neural precursors neurogenesis

Using the anti-NESTIN antibody as a protein marker of neural stem cells, we visualized a decline of these cells in the subgranular zone of the DG (SGZ) of the hippocampus in mice fed with a HFD (**Figure 4**).

Reduction in the activation of apoptotic mechanisms

A reduction in the apoptotic processes was observed using an immunofluorescence against p53 and BCL-2. Thus, by an anti-p53 antibody, a protein associated with tumor suppression, DNA damage and induction of apoptosis, we detected a reduction in the p53 transcription factor of the cytoplasm of different hippocampal neurons in HFD animals in comparison with CT mice (**Figure 5**). The immunofluorescence against BCL-2, which has a role in promoting cellular survival and inhibiting actions of pro-apoptotic proteins, revealed an increase of BCL-2 immunopositive cells in HFD mice versus CT, mainly noticed in the dentate gyrus of the hippocampus. This observed data was supported with the analysis of fluorescence intensity (**Figure 6**).

Autophagy impairment

To analyze if the autophagic activity was altered by HFD mice, we studied the hippocampal distribution pattern of different proteins, such as ULK1 (Serine/threonine-protein kinase 1), LC3 (microtubule-associated proteins light chain 3) and β-catenin. No significant differences in ULK1 immunopositive cells were detected between the experimental animal groups (**Figure 7**). However, the levels of LC3 and β-catenin complexes were reduced in different areas of the hippocampus, such as DG (hilus, molecular and granular layers) and in the *cornu ammonis 1* (CA1) field, specifically in the *stratum lacunosum-moleculare* (slm) and *stratum radiatum* (sr). Quantification of relative fluorescence intensity values reaffirmed the results with a significant decrease on the fluorimetric response on the WT HF experimental group (p value < 0.001). (**Figure 8**).

Discussion

The intent of this experimental work was to support the hypothesis on the link between the development of a metabolic syndrome associated with insulin resistance with sporadic AD. Interestingly, we focused on the role of and neuroinflammatory cellular processes with the reduction in neurogenesis along with the disruption of normal autophagic mechanisms that lead to the appearance of βA depositions in the brain. Overall, this distorted situation that had been reached after a long-life exposure to negative environmental exposure (long-term feeding with a HFD) would promote the development of neuropathological disorders (De Felice, 2013; Heni, 2015).

In order to carry through the present study, we used mice fed with a HFD. The long term feeding of this diet lead to increases in body weight, peripheral hyperglycemia, hyperinsulinemia and insulin resistance together with a mitochondrial dysfunction (Khalyfa, 2013; Takalo, 2014; Petrov, 2015). As members of our group had already described it, the feeding of this diet caused an increase on the concentration of soluble βA in the brain along with the development of memory deficits, supporting the association between metabolic disorders and AD. (Petrov, 2015). In addition, it had also been detected an increase in glial reactivity combined with an escalation in BACE-1 (β-site amyloid precursor protein cleaving enzyme 1) levels, a protein related with the cleavage of the APP peptide. All these data supported an induction of the amyloidogenic pathway in HFD mice as occur with familial AD (Glass, 2010; Lee, 2008; Patil, 2006; Nuzzo, 2015). Our results provide evidence that alterations in specific cellular processes induce the appearance of βA deposits.

One of the cellular mechanism that trigger this situation is the inflammatory response that occurs in the neuronal tissue of the brain (Figure 2 and 3), as a consequence of the alterations in intracellular signaling molecules. Among them, it has been reported that metabolic disorders affect the activity of c-Jun N-Terminal kinase (JNK), protein Kinase R (PKR) and the inhibitor of nuclear factor kappa –B Kinase (IKK). All these enzymes would initiate intracellular cascades that lead to the release of inflammatory mediators into the bloodstream (Nousen, 2013). This situation ends with the disruption of proper blood-brain barrier function making the brain tissue more sensible to outer metabolic alterations (Takeda, 2013).

Park (2010) found that an increase in neuroinflammation affects the progression of neural progenitors within the brain. According to these results, we found a decline in the nestin immunopositive cells in the SGZ, a protein that has a role in the survival and self-renewal of neural stem cells. Consequently, it is suggested that HFD can cause a reduction in the neuronal renovation that affects brain's plasticity and cognitive performance, parameters all decreased in the neuropathology of AD (Singh, 2012).

The down-regulation in HFD-fed animals of LC3 that could form a complex with β-catenin promoting its degradation and enhancing autophagy, pointed out to an alteration in the autophagic system (Jia, 2014). The β-catenin blockade prevents the degradation of p62 and cellular components targeted to the autophagosome, thereby preventing completion of autophagy. This impairment of autophagy was supported with the reduction found in cytoplasmic p53 and an up-regulation of BCL-2 protein, molecules intervene as regulators in several steps on the formation of the autophagosome (Roussy, 2008). This process is important for an adequate regulation of protein homeostasis in neurons. It degrades damaged or unwanted components and recycles those destined for use in energy production and other biosynthetic reactions. Therefore, we can suggest that the increase of βA depositions in the cortex and hippocampus of the elder mice could be the result of a dysfunction of autophagy

(Takechi, 2010). Thus, we theorized that autophagy is involved in the aging of the brain and in age-related neurodegenerative disorders.

To summarize, the observed βA peptide deposition in hippocampus of 16-months old wild-type C57BL/6J mice should not be considered as a spurious observation but, as a signal of how many other systems are distorted, since it is accompanied with significant alterations of cell normal processes, such as increases in neuroinflammation, reduced neural proliferation and decline of autophagy.

Conflict of interest

All authors don't have any actual or potential conflicts of interest including any financial, personal or other relationships with other people or organizations. All authors have reviewed the contents of the manuscript being submitted, approve of its contents and validate the accuracy of the data.

Acknowledgements

OB, MP, AC, ME, EV, and JF belong to 2014SGR 525 from Generalitat de Catalunya.

Bibliography

- Borsini, A., Zunszain, P.A., Thuret, S., Pariante, C.M., 2015. The role of inflammatory cytokines as key modulators of neurogenesis. Trends Neurosci. doi: 10.1016/j.tins.2014.12.006
- De Felice, F.G., Lourenco, M. V., 2015. Brain metabolic stress and neuroinflammation at the basis of cognitive impairment in Alzheimer's disease. Front. Aging Neurosci. 7, 1–8. doi:10.3389/fnagi.2015.00094
- de la Monte, S.M., Wands, J.R., 2008. Alzheimer's disease is type 3 diabetes-evidence reviewed. J Diabetes Sci Technol 2, 1101–1113. doi:10.1177/193229680800200619
- Ettcheto, M., Junyent, F., de Lemos, L., Pallas, M., Folch, J., Beas-Zarate, C., Verdaguer, E., Gómez-Sintes, R., Lucas, J.J., Auladell, C., Camins, A., 2015. Mice Lacking Functional Fas Death Receptors Are Protected from Kainic Acid-Induced Apoptosis in the Hippocampus. Mol. Neurobiol. 52, 120–9. doi:10.1007/s12035-014-8836-0
- Freeman, L.R., Haley-Zitlin, V., Rosenberger, D.S., Granholm, A.-C., 2014. Damaging effects of a high-fat diet to the brain and cognition: a review of proposed mechanisms. Nutr. Neurosci. 17, 241–51. doi:10.1179/1476830513Y.0000000092
- Giacco, F., 2011. Oxidative stress and diabetic complications. Circ Res 107, 1058–1070. doi: 10.1161/CIRCRESAHA.110.223545.Oxidative
- Glass, C.K., Saijo, K., Winner, B., Marchetto, M.C., Gage, F.H., 2010. Mechanisms Underlying Inflammation in Neurodegeneration. Cell 140, 918–934. doi: 10.1016/j.cell.2010.02.016
- Heni, M., Kullmann, S., Preissl, H., Fritsche, A., Häring, H.-U., 2015. Impaired insulin action in the human brain: causes and metabolic consequences. Nat. Rev. Endocrinol. 11, 701–11. doi:10.1038/nrendo.2015.173

- Hristova, M.G., 2013. Metabolic syndrome - From the neurotrophic hypothesis to a theory. Med. Hypotheses 81, 627–634. doi: 10.1016/j.mehy.2013.07.018
- Jia, Z., Wang, J., Wang, W., Tian, Y., XiangWei, W., Chen, P., Ma, K., Zhou, C., 2014. Autophagy eliminates cytoplasmic ??-catenin and NICD to promote the cardiac differentiation of P19CL6 cells. Cell. Signal. 26, 2299–2305. doi: 10.1016/j.cellsig.2014.07.028
- Julien, C., Tremblay, C., Phivilay, A., Berthiaume, L., Émond, V., Julien, P., Calon, F., 2010. High-fat diet aggravates amyloid-beta and tau pathologies in the 3xTg-AD mouse model. Neurobiol. Aging 31, 1516–1531. doi: 10.1016/j.neurobiolaging.2008.08.022
- Khalyfa, a, Carreras, a, Hakim, F., Cunningham, J.M., Wang, Y., Gozal, D., 2013. Effects of late gestational high-fat diet on body weight, metabolic regulation and adipokine expression in offspring. Int. J. Obes. (Lond). 37, 1481–9. doi:10.1038/ijo.2013.12
- Kruiswijk, F., Labuschagne, C.F., Vousden, K.H., 2015. health: a lifeguard with a licence to kill 16. doi:10.1038/nrm4007
- Lee, Y.-H., Tharp, W.G., Maple, R.L., Nair, S., Permana, P. a, Pratley, R.E., 2008. Amyloid precursor protein expression is upregulated in adipocytes in obesity. Obesity (Silver Spring). 16, 1493–500. doi:10.1038/oby.2008.267
- Lim, J., Lachenmayer, M.L., Wu, S., Liu, W., Kundu, M., Wang, R., Komatsu, M., Oh, Y.J., Zhao, Y., Yue, Z., 2015. Proteotoxic Stress Induces Phosphorylation of p62/SQSTM1 by ULK1 to Regulate Selective Autophagic Clearance of Protein Aggregates. PLoS Genet. 11, 1–28. doi: 10.1371/journal.pgen.1004987
- Lipinski, M.M., Zheng, B., Lu, T., Yan, Z., Py, B.F., Ng, A., Xavier, R.J., Li, C., Yankner, B.A., Scherzer, C.R., Yuan, J., 2010. Genome-wide analysis reveals mechanisms modulating autophagy in normal brain aging and in Alzheimer's disease. Proc. Natl. Acad. Sci. 107, 14164–14169. doi:10.1073/pnas.1009485107

- Lorin, S., Pierron, G., Ryan, K.M., Codogno, P., Djavaheri-Mergny, M., 2010. Evidence for the interplay between JNK and p53-DRAM signalling pathways in the regulation of autophagy. Autophagy 6, 153–154. doi:10.4161/auto.6.1.10537
- Maiuri, M.C., Galluzzi, L., Morselli, E., Kepp, O., Malik, S.A., Kroemer, G., 2010. Autophagy regulation by p53. Curr. Opin. Cell Biol. 22, 181–185. doi: 10.1016/j.ceb.2009.12.001
- McGill, A.-T., 2014. Causes of metabolic syndrome and obesity-related co-morbidities Part 1: A composite unifying theory review of human-specific co-adaptations to brain energy consumption. Arch. public Heal. = Arch. belges santé publique 72, 30. doi:10.1186/2049-3258-72-30
- Nousen, E.K., Franco, G.G., Sullivan, E.L., 2013. Unraveling the mechaisms responsible for the comorbidity between metabolic syndrome and mental health disorders. Neuroendocrinology 98, 254–266. doi: 10.1159/000355632.Unraveling
- Nuzzo, D., Picone, P., Baldassano, S., Caruana, L., Messina, E., Marino, A., Cappello, F., Mulè, F., Di, M., 2015. Insulin Resistance as Common Molecular Denominator Linking Obesity to Alzheimer's Disease 1–13.
- Park, K.J., Lee, S.H., Lee, C.H., Jang, J.Y., Chung, J., Kwon, M.H., Kim, Y.S., 2009. Upregulation of Beclin-1 expression and phosphorylation of Bcl-2 and p53 are involved in the JNK-mediated autophagic cell death. Biochem. Biophys. Res. Commun. 382, 726–729. doi: 10.1016/j.bbrc.2009.03.095
- Patil, S., Sheng, L., Masserang, A., Chan, C., 2006. Palmitic acid-treated astrocytes induce BACE1 upregulation and accumulation of C-terminal fragment of APP in primary cortical neurons. Neurosci. Lett. 406, 55–59. doi: 10.1016/j.neulet.2006.07.015
- Pekny, M., Wilhelmsson, U., Pekna, M., 2014. The dual role of astrocyte activation and reactive gliosis. Neurosci. Lett. 565, 30–38. doi: 10.1016/j.neulet.2013.12.071
- Petrov, D., Pedrós, I., Artiach, G., Sureda, F.X., Barroso, E., Pallàs, M., Casadesús, G., Beas-zarate, C., Carro, E., Ferrer, I., Vazquez-carrera, M., Folch, J., Camins, A., 2015. High-fat

diet-induced deregulation of hippocampal insulin signaling and mitochondrial homeostasis deficiencies contribute to Alzheimer disease pathology in rodents. BBA - Mol. Basis Dis. doi: 10.1016/j.bbadis.2015.05.004

- Pistell, P.J., Morrison, C.D., Gupta, S., Knight, A.G., Keller, J.N., Ingram, D.K., Bruce-Keller, A.J., 2010. Cognitive impairment following high fat diet consumption is associated with brain inflammation. J. Neuroimmunol. 219, 25–32. doi: 10.1016/j.jneuroim.2009.11.010
- Roussy, I.G., Roussy, I.G., Paris, U., Paris, U., Paris, S., Paris, S., Federico, N., Federico, N., Biotecnologiche, S., Biotecnologiche, S., Sperimentale, F., Sperimentale, F., Institute, D.T., Institute, D.T., Vergata, T., Vergata, T., 2008. A dual role of p53 in the control of autophagy 1. Autophagy 8627, 810–814. doi:6486 [pii]
- Russell, R.C., Tian, Y., Yuan, H., Park, H.W., Chang, Y., Kim, H., Neufeld, T.P., Dillin, A., Guan, K., 2014. ULK1 induces autophagy by phosphorylating Beclin-1 and activating Vps34 lipid kinase. Nat Cell Biol 15, 741–750. doi: 10.1038/ncb2757.ULK1
- Singh, R.B., Gupta, S., Dherange, P., De Meester, F., Wilczynska, A., Alam, S.E., Pella, D., Wilson, D.W., 2012. Metabolic syndrome: a brain disease. Can J Physiol Pharmacol 90, 1171–83. doi:10.1139/y2012-122
- Stranahan, A.M., 2015. Models and mechanisms for hippocampal dysfunction in obesity and diabetes. Neuroscience 309, 125–139. doi: 10.1016/j.neuroscience.2015.04.045
- Stranahan, A.M., Arumugam, T. V, Cutler, R.G., Lee, K., Egan, J.M., Mattson, M.P., 2008. Diabetes impairs hippocampal function through glucocorticoid-mediated effects on new and mature neurons. Nat. Neurosci. 11, 309–17. doi:10.1038/nn2055
- Takalo, M., Haapasalo, A., Martiskainen, H., Kurkinen, K.M.A., Koivisto, H., Miettinen, P., Khandelwal, V.K.M., Kemppainen, S., Kaminska, D., Mäkinen, P., Leinonen, V., Pihlajamäki, J., Soininen, H., Laakso, M., Tanila, H., Hiltunen, M., 2014. High-fat diet increases tau expression in the brain of T2DM and AD mice independently of peripheral metabolic status. J. Nutr. Biochem. 25, 634–641. doi: 10.1016/j.jnutbio.2014.02.003

- Takechi, R., Galloway, S., Pallebage-Gamarallage, M.M.S., Lam, V., Mamo, J.C.L., 2010. Dietary fats, cerebrovasculature integrity and Alzheimer's disease risk. Prog. Lipid Res. 49, 159–170. doi: 10.1016/j.plipres.2009.10.004
- Takechi, R., Galloway, S., Pallebage-Gamarallage, M.M.S., Wellington, C.L., Johnsen, R.D., Dhaliwal, S.S., Mamo, J.C.L., 2010. Differential effects of dietary fatty acids on the cerebral distribution of plasma-derived apo B lipoproteins with amyloid-beta. Br. J. Nutr. 103, 652–662. doi:10.1017/S0007114509992194
- Takeda, S., Sato, N., Ikimura, K., Nishino, H., Rakugi, H., Morishita, R., 2013. Increased blood-brain barrier vulnerability to systemic inflammation in an Alzheimer disease mouse model. Neurobiol. Aging 34, 2064–2070. doi: 10.1016/j.neurobiolaging.2013.02.010
- Tang, Y., Purkayastha, S., Cai, D., 2015. Hypothalamic microinflammation: A common basis of metabolic syndrome and aging. Trends Neurosci. 38, 36–44. doi: 10.1016/j.tins.2014.10.002
- Tucsek, Z., Toth, P., Sosnowska, D., Gautam, T., Mitschelen, M., Koller, A., Szalai, G., Sonntag, W.E., Ungvari, Z., Csiszar, A., 2014. Obesity in aging exacerbates blood-brain barrier disruption, neuroinflammation, and oxidative stress in the mouse hippocampus: Effects on expression of genes involved in beta-amyloid generation and Alzheimer's disease. Journals Gerontol. - Ser. A Biol. Sci. Med. Sci. 69, 1212–1226. doi:10.1093/gerona/glt177
- Verdile, G., Fuller, S.J., Martins, R.N., 2015. The role of type 2 diabetes in neurodegeneration. Neurobiol. Dis. doi: 10.1016/j.nbd.2015.04.008
- Yoshizaki, T., 2012. Autophagy in Insulin Resistance. Anti-Aging Med. 9, 180–184.

Figure Legends

Figure 1. Stain with Thioflavin-S and 12F4 antibody for the detection of βA fibrillar aggregates and diffuse plaques respectively in coronal hippocampal sections obtained from C57BL/6J 16-months old animals. Images A and B correspond to CT and HFD animals with a Thioflavin-S stain; Detection with 12F4 is shown in images C and D. Comparison between both experimental groups shows presence of several deposits in the DG of the hippocampus in both detection methods. Tissue is also stained with Hoechst (blue). Arrows indicate the presence of the fibrillar aggregates or diffuse plaques. Graphic C shows statistical analysis of the quantification of βA depositions in both the hippocampus and cortex of CT and HFD experimental groups. Statistical analysis was obtained through unpaired Student's t-test with p-value < 0.001. Scale bar represents 200 μm. Abbreviations: mol: molecular layer, gl: granular layer, h: hilus.

Figure 2. Immunofluorescence against GFAP in coronal hippocampal sections obtained from C57BL/6J 16-months old animals. Images A and B correspond to CT and HFD diets respectively. Comparison between A and B reveal that astrocytes (red) of HFD fed animals display higher reactivity (bigger size and more ramified profiles). Tissue is also stained with Hoechst (blue). Scale bar represents 100 μm. Abbreviations: mol: molecular layer, gl: granular layer, h: hilus.

Figure 3. Microglial reactivity observed using an anti-Iba1 antibody (red) in the DG of the hippocampus after a 16-month feeding of a CT and HFD. Images A and B correspond to CT and HFD diets respectively. Comparison between experimental groups shows an increase in the microglial response in the HFD fed animals versus CT. Tissue is also stained with Hoechst (blue). Scale bar represents 100 μm. Abbreviations: mol: molecular layer, gl: granular layer, h: hilus.

Figure 4. Detection of Nestin positive cells counterstained with Hoechst in the DG of the hippocampus from CT and HFD fed animals. Images A and B correspond to CT and HFD diets respectively. Comparison between A and B reveal that in the HFD-fed experimental group there would be a decrease in the fluorescence response both from NPCs in the granular layer (red). Nestin positive cells are indicated in the images with arrows. Graphic C shows a quantification of nestin positive cells in the DG of multiple

animals per group in similar and comparable Bregma areas. Scale bar represents 200 µm. Abbreviations: mol: molecular layer, gl: granular layer, h: hilus**.**

Figure 5. Immunofluorescence against p53 in coronal hippocampal sections obtained from C57BL/6J 16-months old animals. Images A and B correspond to CT and HFD diets respectively. The results reveal a fluorescence response in the cytoplasm of the cells in the CT groups that has nearly disappeared in the HFD fed animals. Tissue is also stained with Hoechst (blue). Graphic C shows statistical analysis of difference in relative fluorescence intensity between CT and HFD experimental groups. Statistical analysis was obtained through unpaired Student's t-test with p-value < 0.0001. Scale bar represents 200 µm. Abbreviations: mol: molecular layer, gl: granular layer, h: hilus.

Figure 6. BCL-2 detection in coronal hippocampal sections obtained from C57BL/6J 16-months old animals. Images A and B correspond to CT and HFD diets respectively. Comparison between A and B reveal that HFD-fed mice have much higher relative fluorescence intensity against BCL-2 protein (green). Tissue is also stained with Hoechst (blue). Graphic C shows statistical analysis of difference in relative fluorescence intensity between CT and HFD experimental groups. Statistical analysis was obtained through unpaired Student's t-test with p-value < 0.0001. Scale bar represents 200 µm. Abbreviations: mol: molecular layer, gl: granular layer, h: hilus**.**

Figure 7. ULK1 positive cells were detected in coronal hippocampal sections obtained from C57BL/6J 16-months old animals. Images A and B correspond to CT and HFD diets respectively. Comparison between A and B show higher relative fluorescence intensity in the HFD experimental group (green). Tissue is also stained with Hoechst (blue). Arrows indicate the presence of ULK1 positive cells in the tissue. Graphic C shows statistical analysis shows no significant differences between CT and HFD experimental groups. Statistical analysis was obtained through unpaired Student's t-test with p-value < 0.0001. Scale bar represents 200 µm. Abbreviations: mol: molecular layer, gl: granular layer, h: hilus.

Figure 8. Representative LC3 and β-catenin detection in coronal hippocampal sections obtained from C57BL/6J 16-months old animals. Images A-E and F-J correspond to CT and HFD diets respectively. From left to right we see in the first column (A and F) immunohistochemistry against LC3 (red), next (B and G) immunohistochemistry against β-catenin (green), next (C and H) Hoechst stain (blue) and lastly, merge

of all three colors (D and I, E and F). Scale bar for images A-D and F-I represents 200 µm. Scale bar for E and J represents 20 µm. There is a reduction in the relative fluorescence response in the HFD animals, in both LC3 and β-catenin, in contrast with CT. Abbreviations: mol: molecular layer, gl: granular layer, h: hilus.

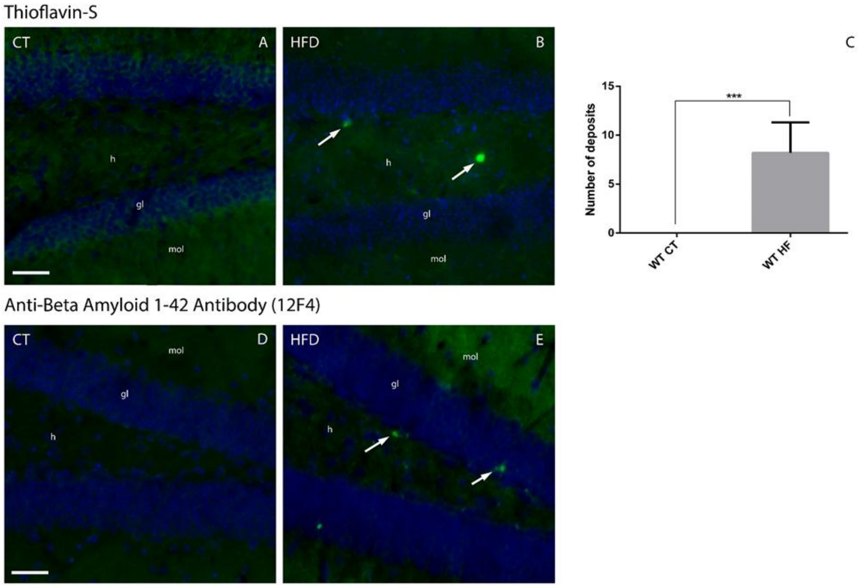
Thioflavin-S
CT
A
HFD
B
C
h
gl
mol
Number of deposits
0
5
10
15
***
WT CT
WT HF
Anti-Beta Amyloid 1-42 Antibody (12F4)
CT
D
HFD
E

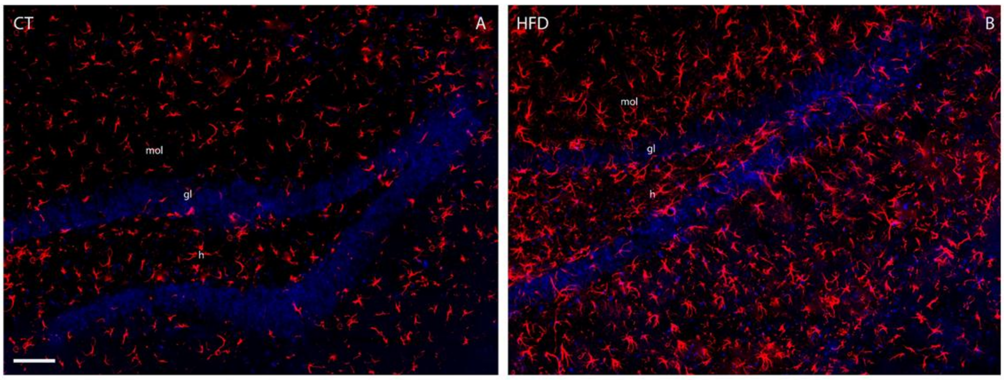
CT
A
mol
gl
h
HFD
B
mol
gl
h

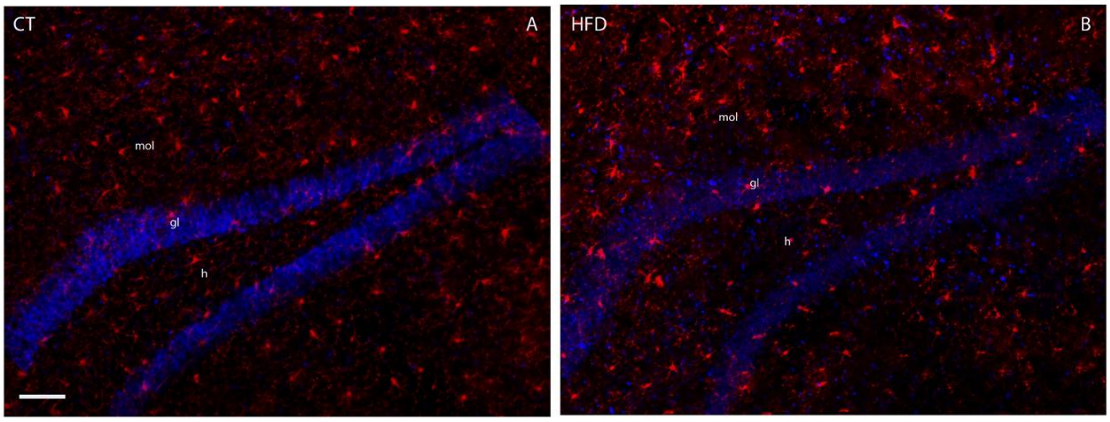
CT
A
mol
gl
h
HFD
B
mol
gl
h

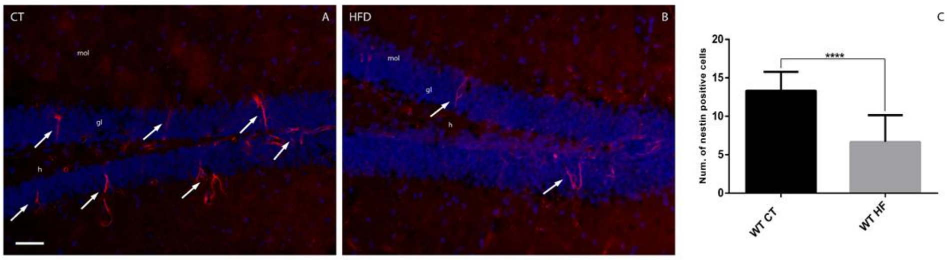

CT
A
mol
gl
h
HFD
B
mol
gl
h
C
Num. of nestin positive cells
20
15
10
5
0
****
WT CT
WT HF

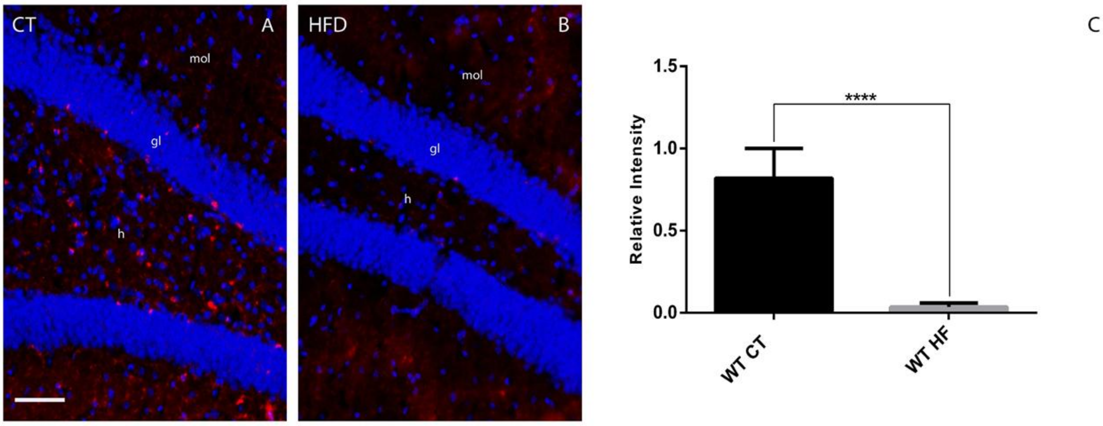
CT
A
mol
gl
h
HFD
B
mol
gl
h
C
1.5
1.0
0.5
0.0
Relative Intensity
****
WT CT
WT HF

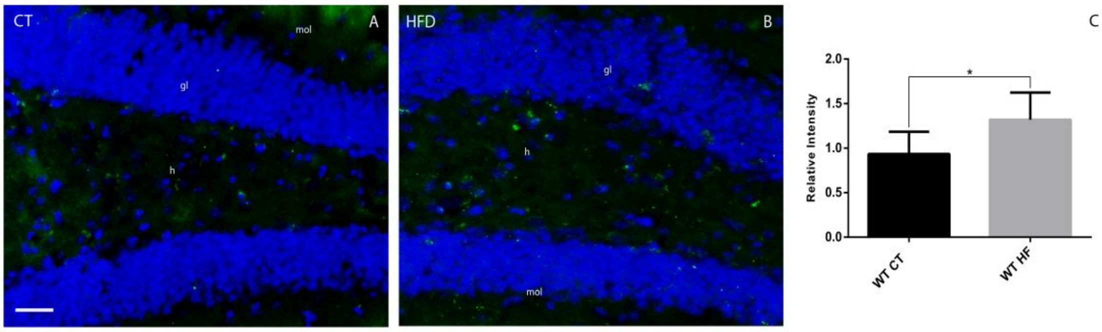
CT
mol
A
gl
h
HFD
B
gl
h
mol
C
2.0
1.5
1.0
0.5
0.0
Relative Intensity
*
WT CT
WT HF

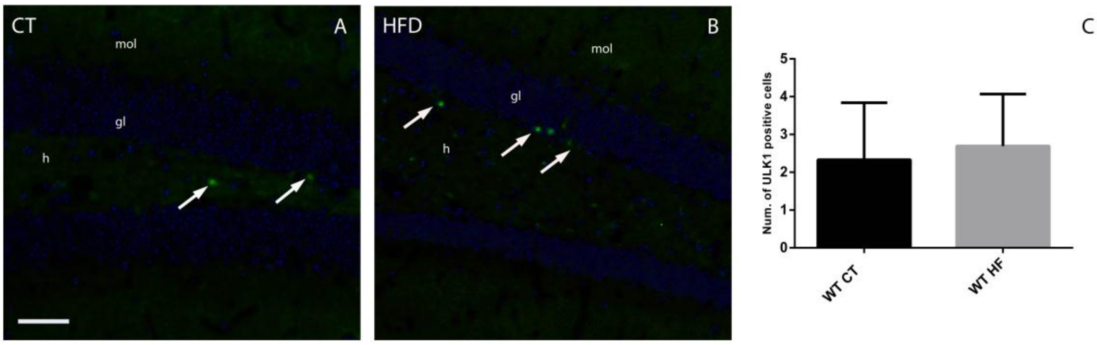
CT
A
mol
gl
h
HFD
B
mol
gl
h
C
Num. of ULK1 positive cells
0
1
2
3
4
5
WT CT
WT HF

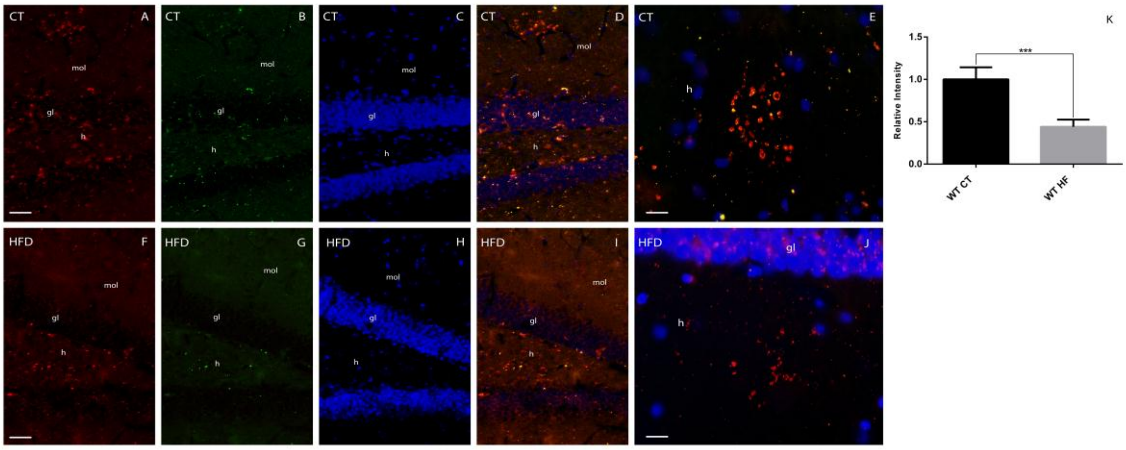
CT
A
mol
gl
h
CT
B
CT
C
CT
D
CT
E
K
1.5
1.0
0.5
0.0
Relative Intensity
***
WT CT
WT HF
HFD
F
HFD
G
HFD
H
HFD
I
HFD
J

Table 1. Description of caloric content of the CT diet versus HFD diet

	CT	HFD
	Kcal %	**Kcal %**
Protein	24.0	16.4
Carbohydrate	58.0	38.6
Fat	18.0	45.0
Total	100.0	100.0
Ingredients		**Kcal**
Casein, 30 Mesh		912
Maltodextrin 10		680
Corn Starch		1424
Soybean Oil		225
Coconut Oil		2277
Vitamin Mix V10001		40
Total		5558

Table 2. List of primary antibodies used in the immunofluorescence procedure.

Primary Antibody	*Reference*	*Company*	*Antigen*	*Source*	*Concentration*
Anti-GFAP	ab7260	Abcam	Glial Fibrillary Acidic Protein	Rabbit	1:1000
Anti-Iba1	019-19741	Wako	Microglia	Rabbit	1:500
Anti-LC3 A/B	ab128025	Abcam	Microtubule-associated protein 1A/1B-light chain 3	Rabbit	1:200
Anti-Nestin	MAB353	Chemicon	Nestin	Mouse	1:200
Anti-ULK1	Ab128859	Abcam	ULK1	Rabbit	1:200
Bcl-2 (N-19)	sc-492	Santa Cruz	B-cell lymphoma 2	Rabbit	1:500
p53 (C-11)	sc-55476	Santa Cruz	p53	Mouse	1:200
β-catenin	sc-1496	Santa Cruz	β-catenin	Goat	1:200
12F4	SIG-39142	BioLegend	β-Amyloid 1-42 peptide	Mouse	1:1000

Table 3. List of secondary antibodies used in the immunofluorescence procedure.

Secondary Antibody	***Reference***	***Company***	***Antigen***	***Source***	***Concentration***
AlexaFluor 594	A11005	Life Technology	Mouse IgG	Goat	1:200
AlexaFluor 594	A11012	Life Technology	Rabbit IgG	Goat	1:200
AlexaFluor 488	A11055	Life Technology	Goat IgG	Donkey	1:200
AlexaFluor 488	A21202	Life Technology	Mouse IgG	Donkey	1:200
AlexaFluor 488	A21206	Life Technology	Rabbit IgG	Donkey	1:200